JOURNAL OF THEORETICAL
AND APPLIED MECHANICS
3, **37**, 1999

NUMERICAL SIMULATION OF ADAPTIVE BONE REMODELING

THOMAS PANDORF*
ABDELKADER HADDI*†
DIETER CHRISTIAN WIRTZ°
JAN LAMMERDING*
RAIMUND FORST°
DIETER WEICHERT*†

* *Institute of General Mechanics, RWTH Aachen, Germany*
† *Laboratoire de Mécanique des Lille (LMLI-EUDIL),*
Université des Sciences et Technologies de Lille, France,
° *Orthopaedic Clinic, RWTH Aachen, Germany*
e-mail: pandorf@iam.rwth-aachen.de

Recent developments in computational mechanics and of high speed digital computers have lead to the implementation of various mathematical continuum models of adaptive bone remodeling depending on the internal bone structure and the loads applied to this structure. In order to study the variation in apparent density and structural anisotropy of the bone due to different loading situations, both mechanical and non-mechanical criteria are taken into account in the presented paper to simulate the bone adaptation behaviour. The mechanical and physiological modeling, its underlying assumptions and numerical implementation into a finite element program is presented. Sample calculation of the proximal femur illustrates the developed model.

Key words: bone adaptation, anisotropy, non-mechanical stimuli

1. Introduction

Bone as a living tissue reacts to environmental influences by changing its external geometry and internal structure. These changes are regulated by physiological processes being influenced by mechanical and non-mechanical

factors, commonly referred to as adaptive bone modeling or remodeling. Remodeling is the coupled process of bone resorption and formation, while modeling means new bone deposition (without prior resorption) or bone resorption (not followed by deposition). Due to the adaptation, a permanent repair and replacement of bone material and exchange of the stored minerals are possible (Vander et al., 1994).

Bones belong to the interstitial tissue (supportive tissue) but differ from other tissues by a high content of inorganic salts giving them a comparatively high strength. Bone cells come to only 5% of the total bone mass. They are classified in osteoclasts, osteoblasts, and osteocytes according to their function and development: osteoclasts absorb bone, osteoblasts form new bone material, and osteocytes are assumed to play an important role in the calcium level regulation (Vander et al., 1994). Macroscopically, the bone structure can be divided into two principal regions of the material disposition: the cortical and cancellous bones. The cortical bone is quite dense compared to the cancellous bone, and its material behaviour may be approximated by an orthotropic and transversely isotropic constitutive model, respectively. The density and orientation of trabecular bone is related to the mechanical loading, i.e. the trabeculae orientation is aligned to the principal stress trajectories resulting from the mean daily load acting on the bone. Therefore, the trabeculae are only subject to tension or compression and almost no bending takes place.

The adaptive process consists of internal remodeling and external remodeling. Internal remodeling describes a change of density and structure, and external remodeling specifies an evolution of the bone shape which redefines the external geometry. Generally, external remodeling develops slowlier than internal remodeling (Weinans et al. 1993). Furthermore, physiological external remodeling is clinically hard to prove because in most cases it is due to pathological circumstances.

The geometrical and material structure of the bone, diversity of the loading (muscles, ligaments etc.) and capability of bone to adapt to changing loading conditions has been studied by numerous authors. Wolff (1892) stated his famous law of transformation, which might be summarized as follows: changing loading conditions will lead to definite changes of shape and internal architecture of bones. One of the first mathematical formulations adopting Wolff's transformation law was given by Pauwels (1965). He assumed that in the fully developed bone tissue an optimal mechanical stimulus S_{norm} had to exist where equilibrium between bone resorption and apposition predominated. If this stimulus is exceeded due to increased mechanical loading bone adaptation takes place, whereas a drop in the mechanical loading leads to bone resorp-

tion. Frost (1964) developed a somewhat modified theory where the medium deformation was taken as a control parameter for bone adaptation. This work was stimulated by clinical observations on shape adaptation in the healing of broken bones.

Beaupré et al. (1990a,b) combined the internal and external adaptation behaviour by taking into account the bone surface as the basis of the remodeling processes. In the interior of the bone, the apparent density increases/decreases whereas on the surface a change of the shape is calculated. As the regulating stimulus, the mean deformation energy density per day is adopted applying a continuum mechanical approach. Similar models have been developed by Huiskes et al. (1987) and Weinans et al. (1989, 1992, 1993). Starting from the isotropic model (cf Beaupré et al., 1990a,b), Jacobs et al. (1997) derived *a formulation for a local control process leading* to global optimality of the structure which is assumed to behave fully anisotropic. The local regulation is assumed to happen on the tissue and cellular level (cf Carter, 1987; Mullender et al., 1994). As optimizing parameter serves the difference between the external power and the internal energy rate due to the adaptation. The time variables are not related to the short-term deformation processes but to the long term adaptation behaviour.

Hart and Davy (1989) formulated a theory for bone adaptation based on the bone cell biology taking into account the cell activation and differentiation as well as the number and activity of osteoblasts and osteoclasts acting on the bone. The activity of the cells is described by a stimulus depending on the mechanical strain, and the resulting adaptation process is determined by the sum of osteoblast and osteoclast activity.

Unlike in the previous models, Prendergast and Huiskes (1996) postulated the bone adaptation as caused by micro damage due to mechanical loading. As damage, the fracture of collagen fibers, micro cracks of the bone lamellae or lamellae debonding are considered. This changes the local deformation behaviour around the lacunae, small gaps in the cortical bone. Accumulating damage finally leads to progressing deformation which then starts the remodeling process.

Pettermann et al. (1997) developed a model where the meso-mechanical structure of the spongious bone is considered. Depending on the stress level, a continuous transition between different shapes of the spongiosa is possible. They are idealized as hexagonal honeycombs (uniaxial stress state), plates (plane stress), and isotropic open cells (multi axial stress state). The direction of microstructural elements is assumed to coincide with the principal stress directions.

Excluding the cited model by Hart and Davy, all approaches to the bone adaptation are purely phenomenological. They describe empirical observations involving only mechanical criteria and neglecting the underlying physiological processes. Nevertheless, the influence of biological factors such as immunological, hormonal, and haemodynamical stimuli on bone adaptation are physiologically combined with the mechanical stimuli. Only if these non-mechanical factors are considered in bone adaptation models, a number of clinically observed bone resorption phenomenae can be explained, e.g. the osteoporosis due to age.

To fill this gap, a model is presented in this paper simulating the bone reaction to changing mechanical and non-mechanical influences. In order to simulate the adaptive modeling and remodeling behaviour of bone due to mechanical influences, the previously mentioned theory of Jacobs et al. (1997) is used. Only changes of the internal structure (density and stiffness matrix changes) are considered. This remodeling theory has been incorporated into an existing finite element program to calculate the remodeling stimulus and stiffness matrix changes. The non-mechanical model has been implemented into a separate numerical code together with the isotropic mechanical model described in this paper. An integrated finite element program covering both the anisotropic mechanical and the non-mechanical model is currently under work.

2. Theoretical framework

2.1. Isotropic bone remodeling

In the present study, no changes of the external form of the bone (shape changes) are considered (Fig.1). Furthermore, the apparent density and the stiffness of the bone are the only descriptors of internal bone remodeling.

A bone is generally subject to external forces causing internal loads and deformations, represented by stresses and strains in the bone material. It is assumed that these stresses or strains are transformed to local mechanical stimuli, sensed by the bone. Following the model by Beaupré (1990a), the tissue stress stimulus ψ_b is introduced, related to the effective stress by

$$\psi_b = \sqrt[m]{\sum_{i=1}^{N} n_i \bar{\sigma}_{b_i}^m} \tag{2.1}$$

Here

N – number of load cases considered
n_i – number of cycles per day for the load case i
$\overline{\sigma}_{b_i}^m$ – true level effective stress of bone tissue
m – empirical weighting exponent.

In the formulation by Beaupré et al. (1990a,b), the bone response is determined from the tissue-level stress stimulus error e

$$e = \psi_b - \psi_{bAS} \tag{2.2}$$

where the attractor stress stimulus ψ_{bAS} is a function of the stress exponent m and the number of cycles of effective stress. It is determined experimentally.

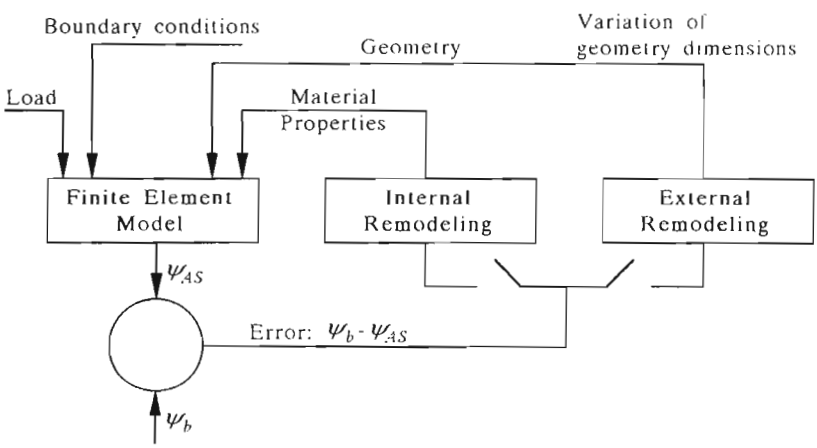

Fig. 1. General model of the bone remodeling criteria

The rate of surface apposition and resorption $\dot{\rho}$ is approximated by the following piecewise linear functions

$$\dot{\rho} = \begin{cases} c(e+w) & \text{for } e < -w \\ c(e-w) & \text{for } e > w \\ 0 & \text{for } -w \leqslant e \leqslant +w \end{cases} \tag{2.3}$$

where c is an empirically obtained constant and w ($w = w_1 = w_2$) is the half-width of the central normal activity region which is called the dead zone or lazy zone (Fig.2). Fig.2 represents this function with a dead zone of the width $w_1 + w_2$.

The bone material is in the first step considered to be isotropic. The elastic modulus as a function of the apparent density can then be approximated by,

e.g. Jacobs et al. (1997)

$$E = b\rho^{\beta} \tag{2.4}$$

where b and β are constants. The new density is defined as

$$\rho(\boldsymbol{x}, T) = \int_{T_0}^{T} \dot{\rho}(\boldsymbol{x}, t)\, dt + \rho(\boldsymbol{x}, T_0) \tag{2.5}$$

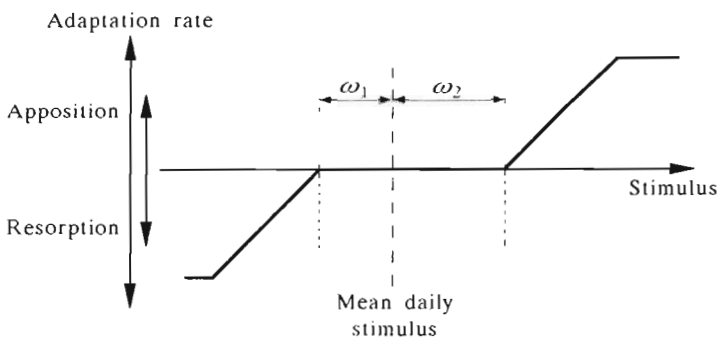

Fig. 2. Relation between the bone apposition or resorption and the remodeling stimulus

2.2. Anisotropic bone remodeling

To account for the entire stress history of an anisotropic bone, a daily remodeling stimulus was proposed by Jacobs et al. (1997)

$$\psi_b = K \frac{\sqrt{\boldsymbol{\varepsilon} : \mathbf{C} : \boldsymbol{\varepsilon}}}{\rho^{2-\beta/2}} \tag{2.6}$$

Here

- β – exponent of the isotropic material model
- $\mathbf{C}, \boldsymbol{\varepsilon}$ – stiffness and strain of the bone material, respectively
- K – function involving several constants, $K = \rho_c^2 \sqrt[m]{n}\sqrt{b}$, where ρ_c, n, m, b are the assumed density of cortical bone, number of loading cycles applied per day, empirical weighting exponent, and constant ($b = 3,79$ for isotropic material), respectively.

The symbol : denotes the double contraction product.

Two criteria can now be formulated to determine the type of remodeling response, one being active in the case of net resorption, and one in the case

of net apposition. As in the isotropic model, w is the half-width of the dead zone (Fig.3).

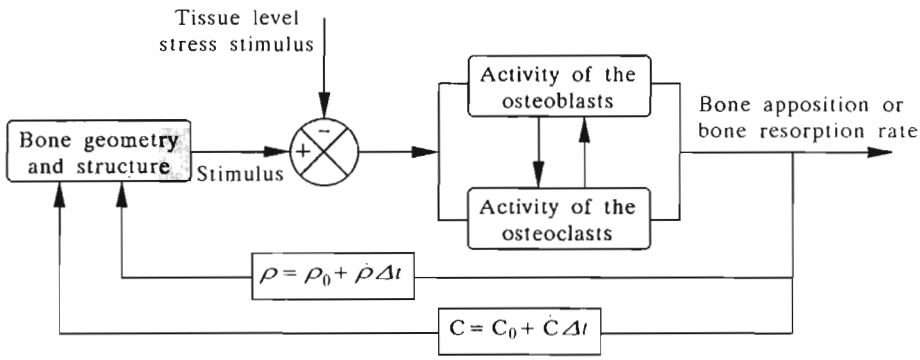

Fig. 3. Concept of the modeling of the adaptation behaviour of bone according to Jacobs et al. (1997)

The three possible situations (net resorption, dead zone and net apposition) lead to changes of the stiffness tensor and density

$$\dot{\mathbf{C}} = \begin{cases} -\gamma^r \dfrac{\boldsymbol{\sigma} \otimes \boldsymbol{\sigma}}{\boldsymbol{\sigma} : \boldsymbol{\varepsilon}} & \text{net resorption} \\ \gamma^a \dfrac{\boldsymbol{\sigma} \otimes \boldsymbol{\sigma}}{\boldsymbol{\sigma} : \boldsymbol{\varepsilon}} & \text{net apposition} \\ \mathbf{0} & \text{dead zone} \end{cases} \tag{2.7}$$

where

- $\boldsymbol{\sigma}$ – Cauchy stress tensor
- $\mathbf{0}$ – fourth-rank zero tensor
- γ^r, γ^a – Lagrange multipliers of net resorption and net apposition, respectively.

For calculation of the rate of the bone density change, a similar expression is used

$$\dot{\rho} = \begin{cases} c(\psi_b - \psi_{bAS} + \omega) S_v(\rho) & \text{net resorption} \\ c(\psi_{bAS} - \psi_b + \omega) S_v(\rho) & \text{net apposition} \\ 0 & \text{dead zone} \end{cases} \tag{2.8}$$

S_v represents the surface area per unit tissue volume of cancellous bone on which remodeling takes place. It is depicted e.g. by Beaupré et al. (1990a,b).

This non-linear material model has been implemented into a finite element code and applied to the three-dimensional model of proximal femur. For each time increment Δt, the density and stiffness can then be recalculated

$$\rho(t + \Delta t) = \rho(t) + \Delta t \dot{\rho}(t)$$
$$\mathbf{C}(t + \Delta t) = \mathbf{C}(t) + \Delta t \frac{\beta \dot{\rho}(t)}{\rho} \frac{\boldsymbol{\sigma} \otimes \boldsymbol{\sigma}}{\boldsymbol{\sigma} : \boldsymbol{\varepsilon}} \tag{2.9}$$

2.3. Non-mechanical stimuli

Additional to mechanical loading of the bones, physiological factors cause bone adaptation, as has been already mentioned. This is due to the fact, that the bones not only have mechanical tasks in the body but also serve as a storage medium for different minerals such as calcium, phosphorus, and others. The control of the calcium balance in the blood has priority over the mechanical stability, i.e. a shortage of calcium leads to bone resorption even if this may endanger the mechanical stability and lead to bone fracture (cf Vander et al., 1994; Klinke and Silbernagel, 1996; Labs and Abbot, 1999; Löffler and Petrides, 1988). Hereinafter, these non-mechanical factors will be referred to as biological stimuli. In this paper, only the main physiological factors of immunological and hormonal nature are addressed, i.e. no changes of the bone structure due to pathological reasons are taken into account.

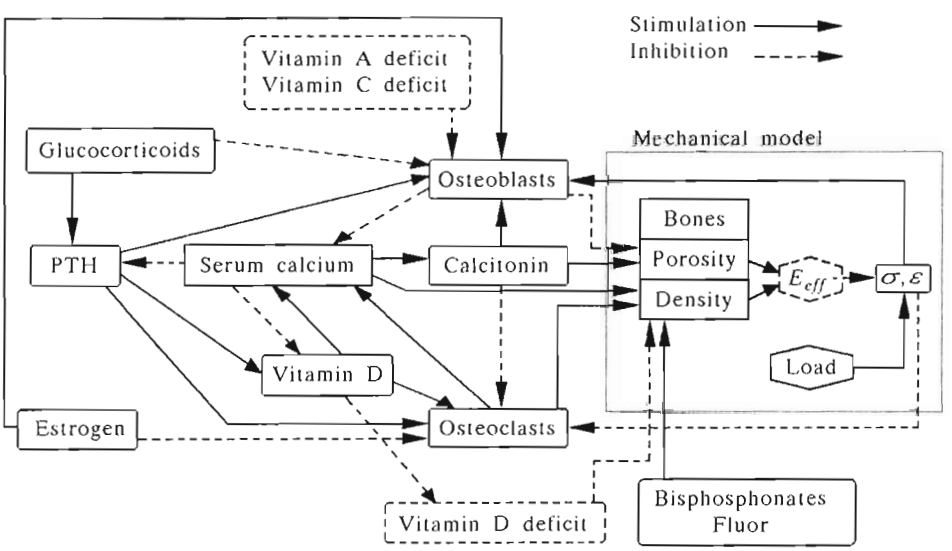

Fig. 4. Scheme of bone remodeling control in humans

In Fig.4, the biological factors considered in this paper and their relations

are depicted. They represent the main biological stimuli acting on the bones (cf Vander et al., 1994; Klinke and Silbernagel, 1996).

Although less than 1% of the whole calcium is found in the blood plasma (cf Vander et al., 1994; Greiling and Gressner, 1995), this concentration is precisely regulated to guarantee the maintenance of vital functions. Besides a control of the calcium intake by food or drugs, mainly the renal excretion regulates the calcium balance (cf Vander et al., 1994; Klinke and Silbernagel, 1996). The most important hormones controlling this balance are the parathormone (PTH) and calcitriol (cf Vander et al., 1994; Greiling and Gressner, 1995; Klinke and Silbernagel, 1996). Short-term fluctuations of the calcium concentration in the plasma are regulated by the exchange of calcium ions with certain tissue cells or a part of the calcium stored in the bone. To regulate long-term calcium deficiency, the lacking calcium is obtained from the hydroxyl apatite which is the not directly water soluble fraction of mineralized bone. For this reason, the osteoclasts are activated to an increased extent leading to a progressing loss of bone mass (cf Labs and Abbot, 1999). Phosphorus in the chemical form of phosphate is also a main part of the hydroxyl apatite. Chemical interactions between the calcium and the phosphate ions and their constant solubility product lead to a rise in the phosphate concentration due to a drop of the calcium concentration and vice versa. Due to multiple functions of phosphate and calcium in the body, this interaction is an important feature of bone adaptation. For a complete description of the dependencies see Vander et al. (1994), Greiling and Gressner (1995), Klinke and Silbernagel (1996).

3. Numerical model

3.1. Mechanical model

The finite element model utilized in the present study is shown in (Fig.6). This model consists of 3324 solid parabolic tetrahedron elements and 6034 nodes. The loading history in the isotropic case is approximated by the three load cases used by Beaupré et al. (1990a,b) (Table 1) representing an equivalent daily load. They consist of distributed loads acting over the joint surface and on the greater trochanter representing the abductor attachment. For the anisotropic model, only a single load is considered (cf Jacobs et al., 1997). The simulation starts with the assumption of homogeneous bone density of $\rho = 1000\,\mathrm{kg\,m^{-3}}$ and initial material coefficients (Young modu-

lus $= 3.79\,\rho^3$ and Poisson ratio $= 0.2$). The parameters required for the calculation of the density change are (Beaupré et al., 1990b): attractor stress stimulus $\psi_{bAS} = 1.2 \cdot 10^6$ Pa, rate constant $c = 8 \cdot 10^{-13}$ (m/day)/(Pa/day), dead zone half-width $w = 1000$ Pa/day and empirical weighting exponent $m = 4$.

Tabele 1. Assumed values for the different applied load sets

Load case	Cycles per day	Magnitude (Joint) [N]	Magnitude (Abductor) [N]
1	6000	2317	703
2	2000	1158	351
3	2000	1548	468

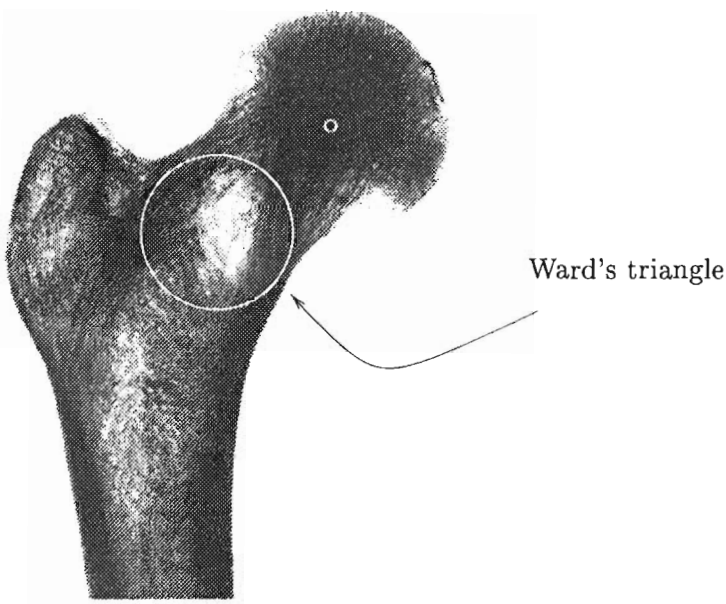

Fig. 5. Natural density distribution and Ward's triangle

After calculation of stresses in the initial homogeneous model, one obtains by virtue of Eq (2.1) the actual stress stimulus in each bone element. The tissue level stress stimulus error e, Eq (2.2), then locally drives the remodeling response, generating a value for the rate apposition or resorption for each element. By calculating the rate of change of the density and the Young moduli for isotropic material, the stiffness tensor in anisotropic material are updated based on Eq (2.3) and Eqs (2.7), (2.8), respectively. The new values of the density and the stiffness tensor are obtained using Eqs (2.5), (2.9) and then

applied to the next time increment of the isotropic model.

Fig.7 shows the computed density distribution compared to a radiogram of the natural femur (Fig.5). Low density regions are observed at the extreme edges of the joint surface and in the proximal region known as Ward's triangle. This behaviour was also observed by Harrigan and Hamilton (1994), Jacobs et al. (1997), and Weinans et al. (1992).

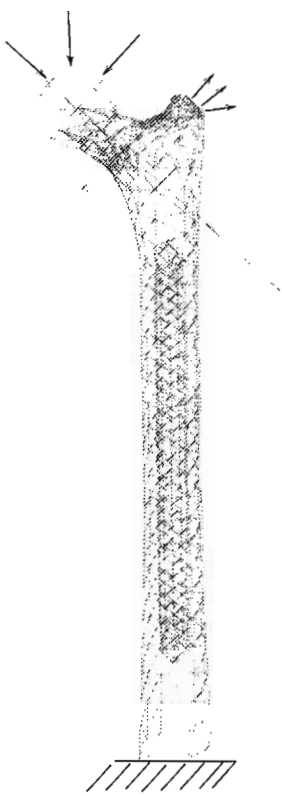

Fig. 6. Finite element model of the femur

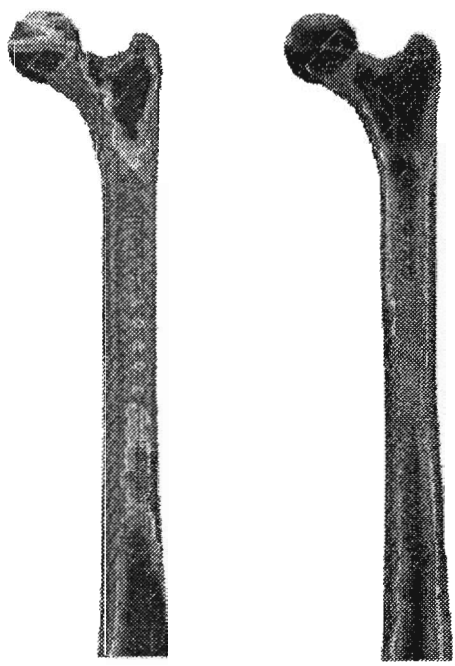

Fig. 7. Calculated density distribution after 13 and 19 iterations, respectively

In the anisotropic case, the principal directions of the stiffness of cancellous bone coincide with the direction of loading (Fig.9). In Fig.8, the degree of anisotropy in the distal part of the bone is higher than that observed by Jacobs. The results obtained for the parameters ($\psi_{bAS} = 2.0 \cdot 10^6$ Pa, $c = 8 \cdot 10^{-11}$ (m/day)/(Pa/day)) are depicted in Fig.8 and are in good agreement with qualitative expectations from observations of trabecular alignment (Fig.5).

However, quantitative evaluation of the results is difficult due to large variation of the material properties of real cancellous bones.

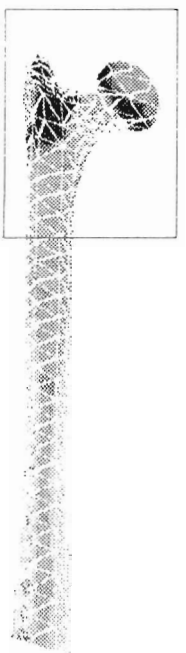

Fig. 8. Calculated stiffness distribution after 10 iterations

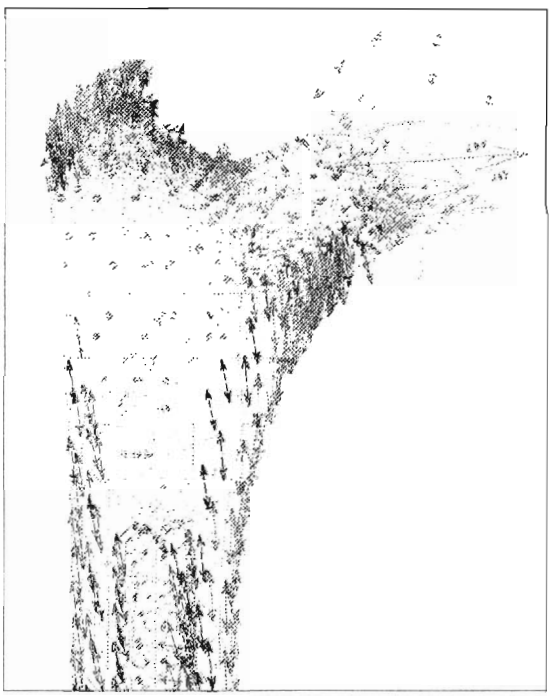

Fig. 9. Calculated stiffness direction after 10 iterations

3.2. Non-mechanical model

The non-mechanical bone adaptation model was implemented into a program where each time increment represents one day. After calculation of the continuum mechanical stresses and strains, the adaptation algorithm first calculates the physiological values of the calcium and phosphate homeostasis. This implies calculation of the plasma concentration of calcium and phosphate as well as of the calciotropic hormones PTH, calcitonin, and calcitriol having a significant influence on bone adaptation. To determine these values, the calcium and phosphate levels due to physiological control are calculated de-

pending on the appropriate plasma concentration

$$Ca = \frac{Calcium_{ECF}}{V_{Pl} + V_{ISF} \cdot GDF_{Ca2+} \cdot fp_{Ca}}$$
$$P = \frac{Phosphor_{ECF}}{V_{Pl} + V_{ISF} \cdot GDF_{Phosphate} \cdot fp_{Phosphate}} \tag{3.1}$$

Here, x_{ECF} is the level of element x in the extracellular fluid, V_{Pl} and V_{ISF} denote the volume of plasma and interstitial fluid, respectively. GDF_x denote the appropriate Gibbs-Donnan-factors ($Ca^{2+} : 0.9/phosphate : 1.09$), and fp is the filterable part of the calcium (60%) and phosphate (90%), respectively. In an iterative process, the steady-state condition is determined, i.e. the mass fluxes have to be balanced. These mass fluxes are the daily intake and excretion as well as the exchanged portion due to bone apposition/resorption.

As already mentioned, the PTH is the most important hormone to control the calcium homeostasis. To determine its plasma concentration, the following equation is proposed

$$PTH = PTH_{norm} + Sec_{PTH}(\Delta Ca^{2+}) + c_{PTH,phosphate} \cdot \Delta phosphate + \ldots \tag{3.2}$$

where PTH_{norm} is the normal PTH concentration (3.0 pmol/l), $Sec_{PTH}(\Delta Ca^{2+})$ is the PTH secretion due to deviations of the calcium level (Löffler and Petrides, 1988), $c_{PTH,x}$ is a weight factor for the PTH secretion triggered by substance x (here phosphate), and Δx is the normalized deviation of substance x from the normal value. The dots indicate that more factors influencing the PTH level might be included. At the present stage of research, only phosphate is considered in our model. The linear form of the equation is assumed as the first approximation to the natural dependencies. For a complete derivation of the foregoing equations, the reader is referred to Lammerding (1999) and to a forthcoming paper.

After reaching the steady state condition, the non-mechanical stimulus for bone adaptation corresponds to the deviation of the calciotropic hormones and the calcium and phosphate ions from the normal plasma level

$$\psi_{nm} = f(PTH,\ calcitriol,\ calcitonin,\ calcium,\ phosphate, \ldots) \tag{3.3}$$

Here, ψ_{nm} denotes the non-mechanical bone stimulus. It is then superposed with ψ_b derived in Section 2.2 to yield the adaptation behaviour. Two examples illustrate the proposed method. The first one is taken from the medical literature (cf Fardellone et al., 1998).

3.2.1. Example 1

An additional daily intake of 1200 mg (30 mmol) calcium for a period of 100 days has been assumed. Both mechanical and non-mechanical bone adaptation models are considered. From Fig.10, it is obvious that both the plasma calcium and the plasma phosphate level adapt to a new situation by reaching a new steady-state level that differs from the nominal value. The additional intake is mainly excreted, and by a small fraction absorbed by the bone. The deviation of the steady-state level of plasma concentration from the nominal value is necessary to trigger these compensatory effects. This can be explained by the proportional control-like behaviour of the calcium homeostasis within the human body requiring a deviation of the steady-state level from the normal level. This regulation is very sensitive so that even small changes in the calcium plasma concentration cause large adjustments in the renal and intestinal functions (cf Greger and Windenhorst, 1996). The densities of cortical and spongious bone (see Fig.11) also increase until they reach a new steady-state level. It can be considered as an equilibrium between the adversatory mechanical and non-mechanical bone remodeling. The non-mechanical adaptation is due to the role of bone as a calcium storage medium leading to a higher bone density. This causes a stiffer bone resulting in a decreased mechanical stimulus that favours bone resorption.

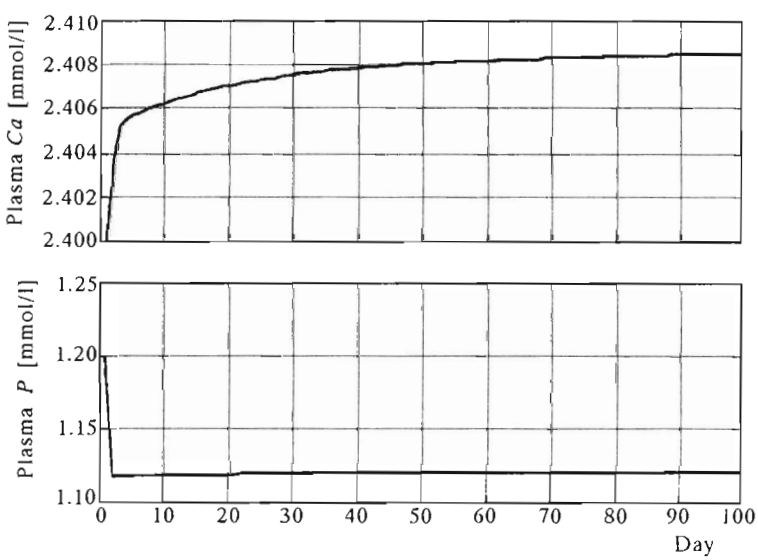

Fig. 10. Development of the plasma calcium and plasma phosphate

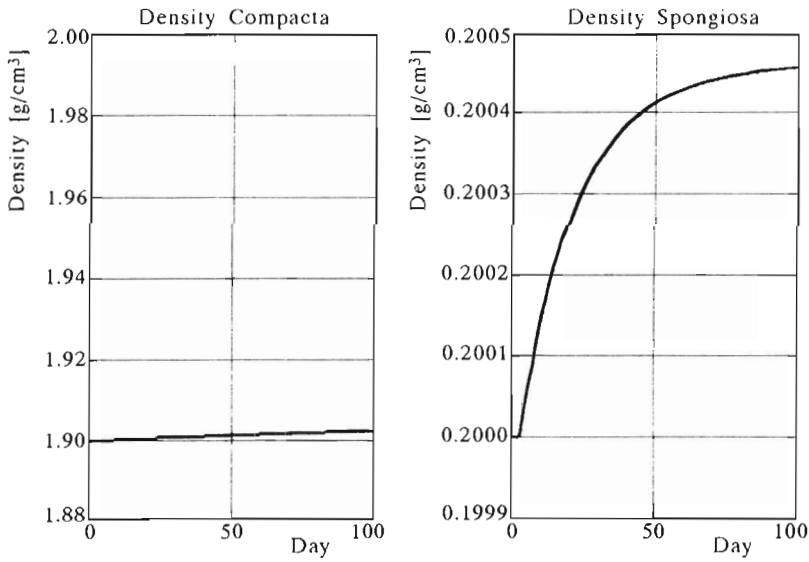

Fig. 11. Density evolution in the cortical and spongious bones, respectively

3.3. Example 2

A stepwise increase of phosphate intake is assumed over a period of four weeks (see Table 2). The first increase takes place after 3 days. The normal intake is 36 mmol/day. Both mechanical and non-mechanical bone adaptation models is considered. The mechanical loading was assumed to be in the adaptation equilibrium at the beginning of the simulation.

Table 2. Values of the daily intake of phosphate

1. week	50 mmol/day
2. week	68 mmol/day
3. week	85 mmol/day
4. week	100 mmol/day

It can be seen in Fig.12 and Fig.13 that an increase of phosphate leads to an increase of bone density. When the amount of phosphate intake further increases, the previously mentioned drop of calcium ions in the plasma leads to bone resorption and, hence, to a loss of bone material. On the other hand, the loss/gain of bone mass results in an increase/decrease of the energy density. This triggers the mechanical adaptation to partly compensate this mass change. In this example, these changes are quantitatively small. Since in real life these changes are often sustained for a long time (significantly more

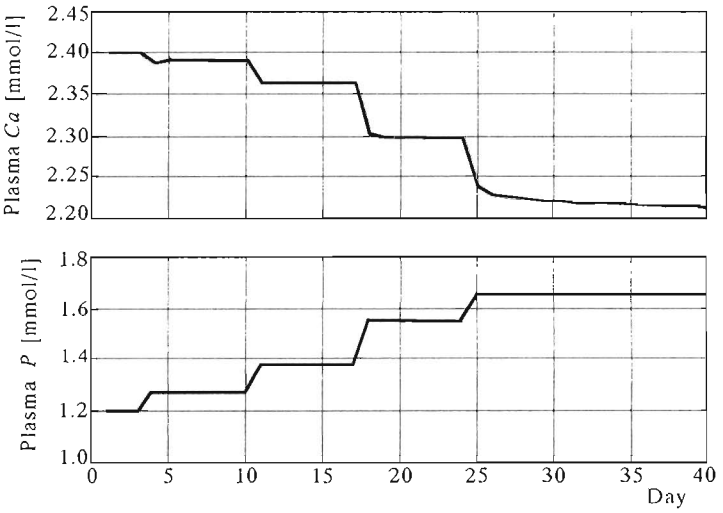

Fig. 12. Development of the plasma calcium and plasma phosphate

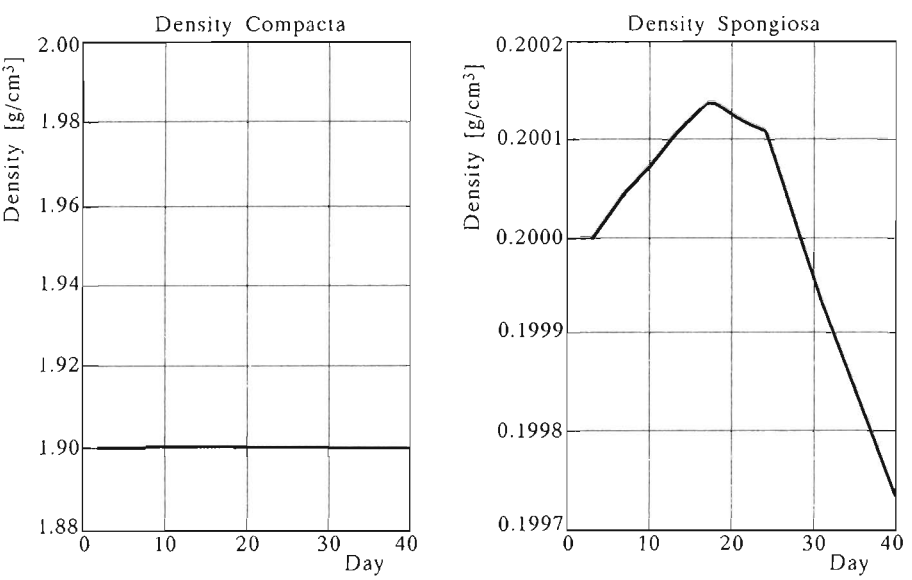

Fig. 13. Density evolution in the cortical and spongious bones, respectively

than one year) the effects on bone mass accumulate and result in considerable variations of bone density.

4. Conclusions

In the present study, a model simulating internal bone adaptation is presented involving mechanical and non-mechanical factors. The mechanical part is based on the assumption that the bone is driven to satisfy Carter's density remodeling criterion. Two criteria are adopted: The first one assumes isotropic material behaviour, and the second criterion is based on the anisotropic stiffness tensor evolution. Three assumptions are adopted in this application of the remodeling theory. The first is the limitation to internal remodeling. The second is the use of the trilinear form of the remodeling law up to certain bounds. In the third assumption, the initial distribution of bone apparent density was assumed to be homogeneous. The anisotropic theory developed in this study is based on the remodeling mechanism taken from the isotropic case. The results obtained for the upper part of the femur including Ward's triangle correspond with the observed natural bone structures. Also, the model predicts quite well the anisotropy in the regions of lower bone. Nevertheless, a reduced stiffness is observed in the compact bone compared with the natural bone. Also, the results do not accurately predict the measured material behaviour of cortical bone. This may be explained by the choice of boundary conditions, small number of finite elements and assumption of initially homogeneous density distribution. Additionally, the reduced number of muscles acting on the femur considered in this paper may be the reason for errors in the calculation of density distribution and stiffness directions. The non-mechanical model involves only those biological stimuli which are considered to exert an important influence on bone adaptation. It is assumed that they equally affect all bones in the body. To verify the presented implementation, a simulation of clinical studies have been carried out showing that the observed clinical behaviour can be predicted. An implementation of the physiological algorithm into the finite element model and a connection with the anisotropic mechanical model yet has to be done.

Acknowledgments

The authors are grateful for the support by the START-program, granted by the hospital complex of the RWTH Aachen.

References

1. BEAUPRÉ G.S., ORR T.E., CARTER D.R., 1990a, An Approach for Time-Dependent Bone Modeling and Remodeling – Theoretical Development, *J. Orth. Res.*, **8**, 5, 651-661
2. BEAUPRÉ G.S., ORR T.E., CARTER D.R., 1990b, An Approach for Time-Dependent Bone Modeling and Remodeling – Application: A Preliminary Remodeling Simulation, *J. Orth. Res.*, **8**, 5, 662-670
3. CARTER D.R., 1987, Mechnical Loading History and Skeletal Biology, *J. Biomechanics*, **20**, 11, 1095-1109
4. FARDELLONE P. ET AL., 1998, Biomechanical Effects of Calcium Supplementation in Postmenopausal Women: Influence of Dietary Calcium Intake, *Am. J. Clin. Nutr.*, **67**, 6, 1273-1278
5. FROST H.M., 1964, *The Laws of Bone Structure*, Charles C. Thomas, Springfield, IL
6. GREILING H., GRESSNER A.M., 1995, *Lehrbuch der Klinischen Chemie und Pathobiochemie*, Schattauer Verlag, Stuttgart New York, 3. Edition
7. GREGER R., WINDENHORST U., 1996, *Comprehensive Human Physiology – from Cellular Mechanisms to Integration*, Vol. 2, Springer Verlag, Berlin, Heilderberg, New York
8. HART R.T., DAVY D.T., 1989, Theories of Bone Modeling and Remodeling, In Cowin S.C. (edit.): *Bone Mechanics*, 253-277, CRC Press, Boca Raton, FL.
9. HARRIGAN T.P., HAMILTON J.J., 1994, Bone Remodeling and Structural Optimization, *J. Biomechanics*, **27**, 3, 323-328
10. HUISKES R., WEINANS H., GROOTENBOER H., 1987, Adaptive Bone-Remodeling Theory Applied to Prosthetic Design Analysis, *J. Biomechanics*, **22**, 1135-1150
11. JACOBS C.R., SIMO J.S., BEAUPRÉ G.S., CARTER D.R., 1997, Adaptive Bone Remodeling Incorporating Simultaneous Density and Anisotropy Considerations, *J. Biomechanics*, **30**, 6, 603-613
12. KLINKE R., SILBERNAGEL S., 1996, *Lehrbuch der Physiologie*, Georg Thieme Verlag, Stuttgart, New York
13. LABS, ABBOTT, 1999, *The Osteo Dynamica Manual*, http://www.abbottrenalcare.com/manual/intro.html
14. LAMMERDING J., 1999, Simulation der Knochenanpassung unter Berücksichtigung mechanischer und nicht-mechanischer Einflussfaktoren, Diplomarbeit, Institut für Allgemeine Mechanik, RWTH Aachen, Accessible under http://www.iam.rwth-aachen.de/Forschung/lammer.html

15. LÖFFLER G., PETRIDES P.E., 1988, *Physiologische Chemie*, Springer Verlag, Berlin, Heilderberg, New York

16. MULLENDER M.G., HUISKES R., WEINANS H., 1994, A Physiological Approach to the Simulation of Bone Remodeling as a Self-Organizational Control Process, *J. Biomechanics*, **27**, 11, 1389-1394

17. PAUWELS F., 1965, *Gesammelte Abhandlungen zur funktionellen Anatomie des Bewegungsapparates*, Springer Verlag, Berlin

18. PRENDERGAST P.J., HUISKES R., 1996, Microdamage and Osteocyte-Lacunae Strain in Bone: A Microstructural Finite Element Amalysis, *J. Biomechanics*, **118**, 240-246

19. PETTERMANN H.E., REITER T.J., RAMMERSTORFER F.G., 1997, Computational Simulation of Internal Bone Remodeling, *Arch. Comp. Meth. Eng.*, **4**, 4, *295-323*

20. VANDER A.J., SHERMAN J.H., LUCIANO D.S., 1994, *Human Physiology*, McGraw-Hill inc., New York

21. WEINANS H., HUISKES R., GROOTENBOER H.J., 1989, Convergence and Uniqueness of Adaptive Bone Remodeling, *Trans. Orth. Res. Soc.*, **14**, 310

22. WEINANS H., HUISKES R., GROOTENBOER H.J., 1992, Effects of Material Properties of Femoral Hip Components on Bone Remodeling, *J. Orth. Res.*, **10**, 6, 845-853

23. WEINANS H., HUISKES R., VAN RIETBERGEN B. ET AL., 1993, Adaptive Bone Remodeling Around Bonded Noncemented Total Hip Arthoplasty: A Comparison Between Animal Experments and Computer Simulation, *J. Orth. Res.*, **11**, 4, 500-513

24. WOLFF J., 1892, *Das Gesetz der Transformation der Knochen*, Hirschwald Verlag, Berlin

Numeryczna symulacja adaptacyjnej przebudowy kości

Streszczenie

Rozwój metod komputerowych mechaniki i szybkich komputerów cyfrowych pozwolił na implementację różnych kontynualnych modeli matematycznych adaptacyjnej przebudowy kości uwzględniających wewnętrzną strukturę kości i obciążenia. W celu zbadania zmian gęstości pozornej i strukturalnej anizotropii kości spowodowanych różnymi obciążeniami, w niniejszej pracy uwzględniono zarówno mechaniczne jak

i niemechaniczne kryteria dla symulacji adaptacyjnego zachowania się kości. Przedstawiono modelowanie mechaniczne i fizjologiczne, związane z tym założenia oraz implementację numeryczną przy pomocy metody elementów skończonych. Dla ilustracji opracowanego modelu przedstawiono wyniki obliczeń dotyczące końca bliższego kości udowej.

Manuscript received March 24, 1999; accepted for print April 27, 1999